CRYSTAL GROWTH & DESIGN

pubs.acs.org/crystal

Article

The Effect of Chain Length and Conformation on the Nucleation of Glycine Homopeptides during the Crystallization Process

Published as part of a Crystal Growth and Design virtual special issue Celebrating John N. Sherwood, Pioneer in Organic and Molecular Crystals

Mingxia Guo, Marie J. Jones, Racheal Goh, Vivek Verma, Emily Guinn, and Jerry Y. Y. Heng*

Cite This: *Cryst. Growth Des.* 2023, 23, 1668−1675

Read Online

ACCESS | Metrics & More | Article Recommendations | Supporting Information

ABSTRACT: To explore the effect of chain length and conformation on the nucleation of peptides, the primary nucleation induction time of glycine homopeptides in pure water at different supersaturation levels under various temperatures has been determined. Nucleation data suggest that longer chains will prolong the induction time, especially for chains longer than three, where nucleation will occur over several days. In contrast, the nucleation rate increased with an increase in the supersaturation for all homopeptides. Induction time and nucleation difficulty increase at lower temperatures. However, for triglycine, the dihydrate form was produced with an unfolded peptide conformation (pPII) at low temperature. The interfacial energy and activation Gibbs energy of this dihydrate form are both lower than those at high temperature, while the induction time is longer, indicating the classical nucleation theory is not suitable to explain the nucleation phenomenon of triglycine dihydrate. Moreover, gelation and liquid−liquid separation of longer chain glycine homopeptides were observed, which was normally classified to nonclassical nucleation theory. This work provides insight into how the nucleation process evolves with increasing chain length and variable conformation, thereby offering a fundamental understanding of the critical peptide chain length for the classical nucleation theory and complex nucleation process for peptides.

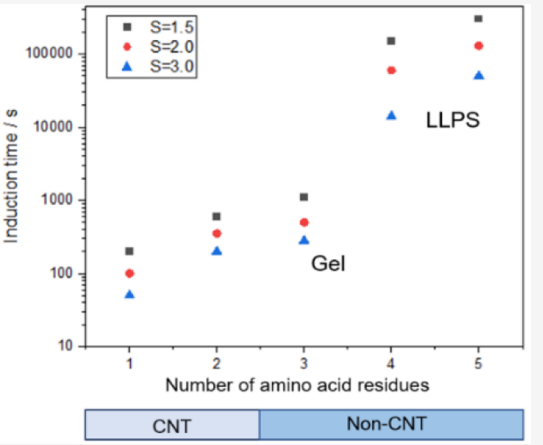

INTRODUCTION

Nucleation is the first and essential step in the process of crystallization, where a new thermodynamic phase forms with lower free energy.[1] Nucleation kinetics plays a decisive role in the control of polymorphism and crystalline product quality.[2] The current crystal nucleation research can be explained through classical and nonclassical nucleation theories.[3−6] Among them, the classical nucleation theory remains the most common theoretical model for the understanding of nucleation, which suggests that concomitant density and order fluctuations cause the formation of clusters, and following that clusters begin to aggregate to form the nucleus.[7,8] The nucleation process of macromolecule crystallization has been explored by numerous pathways in the past decade.[9,10] With complex secondary, tertiary, and quaternary structures, classical nucleation theory which can be applied well to explain small molecule nucleation has encountered a formidable obstacle in regard to proteins. Nonclassical nucleation theories, such as the two-step theory and the prenucleation clusters theory, have been proven to explain a specific protein nucleation process.[11−14] Therefore, these theories put forward questions such as, what is the critical chain length of peptides to distinguish these two different nucleation theories? Is there any relationship between the conformation and the nucleation mechanism?

Peptides are structurally comparable to proteins due to the presence of peptide bonds and amino acid residues, but most of them have a simpler space structure without any tertiary and quaternary structure. Additionally, the short chain length makes it looks like small molecules in molecular size. Therefore, peptides serve as an excellent model for studying the crucial chain length at which classical nucleation occurs. Few studies have been conducted on the nucleation mechanism for peptides, making it imperative to determine the link between small molecule nucleation and protein nucleation.

Received: November 1, 2022
Revised: January 9, 2023
Published: January 24, 2023

https://doi.org/10.1021/acs.cgd.2c01229
Cryst. Growth Des. 2023, 23, 1668−1675

Glycine is the simplest amino acid with a single hydrogen atom as its side chain, allowing study on the nucleation of glycine homopeptides to be conducted without concerning the effect of side chains. The solubilities of glycine homopeptides (from mono- to pentaglycine) were measured using UV−vis in our previous work.[15] In another work, triglycine was found to form a dihydrate with unfolded pPII (polyproline II) conformation under 303 K.[16] Based on these thermodynamic and morphological research studies, the primary nucleation induction time of glycine homopeptides at different supersaturation levels (1.4 to 2.4) and temperatures (278.15 K and 283.15 K) was investigated to determine the effect of peptide chain length and conformation on the nucleation of peptide crystallization. At each condition, 100 experiments have been conducted to capture the statistics of the nucleation process. The data were analyzed using the probability distribution function of the induction time within the framework of classical nucleation theory. Overall, the nucleation parameters (nucleation rate J, growth time t_g, interfacial energy γ, critical radius: r_C, number of molecules in critical nucleus n_C, and activation Gibbs energy ΔG_C) of glycine homopeptides have been calculated and compared.

THEORY

Induction Time t_d. Before a nucleus can be detected by instruments or human vision, it must have reached a certain size or be present in a large number, which means that the time t_n for a single nucleus to be formed cannot be accurately recorded. The period of time between the moment of a constant supersaturation created and the formation of crystals which can be detected is defined as "induction time" (t_d).[5] The nuclei have to grow to a detectable size in order to obtain measurements since it is impossible to detect the real induction time (t_n) when the critical nuclei form. Due to this, evaluating "induction time" is the only way. Induction time is larger than t_n and cannot be regarded as a fundamental characteristic of the system because its values depend on the method used to identify the emergence of a new phase. Examining the values for induction time, however, can help comprehend the mechanisms of new phase formation and growth from critical nuclei into crystals.[17]

The induction time can be expressed as the sum of three terms as follows:

$$t_d = t_{tr} + t_n + t_g \tag{1}$$

where t_d is the measured induction time, t_{tr} is the time needed for reaching steady-state nucleation, t_n is the nucleation time, and t_g is the growth time required for the critical nucleus to grow to a larger detected size.

By determining the induction time, the nucleation kinetics can be calculated and used to find the thermodynamic and kinetic parameters (such as interfacial energy, critical nucleation free energy, pre-exponential factor, and critical radius and number of molecules in the nucleus) required for efficient crystallization design which will be beneficial for future works in crystallization.

Determination of Nucleation Rate J. Due to the stochastic nature of crystallization, the measured induction times of glycine homopeptides can be approximated to a cumulative probability distribution $P(t)$. For N isolated experiments, the probability $P(t)$ of observing an induction time between time zero and t is defined as follows:

$$P(t) = \frac{n(t)}{N} \tag{2}$$

where $n(t)$ is the number of trials for which crystals were detected at time t.

The experimentally determined cumulative probability distribution for the induction times was found by Jiang and ter Horst to resemble the Poisson Distribution.[18] They have indeed expressed the probability of finding at least one nucleus at time t_n as the Poisson distribution:

$$P(t_n) = 1 - \exp(-JVt_n) \tag{3}$$

where J is the nucleation rate and V is the volume of solution.

Besides, the probability distribution for the detection time can thus be rewritten on the model of the Poisson Distribution as eq 4. The transient period t_{tr} can be ignored here since it is unimportant in aqueous solutions of moderate supersaturations and viscosities.[19]

$$P(t_d) = 1 - \exp(-JV(t_d - t_g)) \tag{4}$$

Nucleation Data Derived from Classical Nucleation Theory. The Classical Nucleation Theory was used to determine the thermodynamic factor B from which nucleation data can be derived and compared for each glycine homopeptide.

The supersaturation S can be expressed as

$$S = \frac{C}{C^*} \tag{5}$$

where c is the actual concentration of the solution, c^* is the solubility at the specific temperature, and the unit of all data is mole fraction.

The relation between the nucleation rate J, the induction time obtained experimentally, and supersaturation S could be expressed as the following equations based on different limiting steps:[20−22]

$$\ln J = \ln A - \frac{B}{\ln^2 S} \tag{6}$$

$$\ln\left(\frac{J}{S}\right) = \ln A - \frac{B}{\ln^2 S} \tag{7}$$

$$\ln\left(\frac{J}{S\ln(S)}\right) = \ln A - \frac{B}{\ln^2 S} \tag{8}$$

$$\ln J + 3\ln(\ln S) = \ln A - \frac{B}{\ln^2 S} \tag{9}$$

where A and B are usually considered to be constants, and the exponent $B/\ln 2\ S = W/kT$ is the dimensionless nucleation energy barrier for nucleation.

Equations 6 and 7 is for interface-transfer control, eq 8 is for volume-diffusion control, and eq 9 is another interface-transfer control expression according to the assumption that nucleus growth takes place by a surface nucleation mechanism. Equation 9 was plotted for each polyglycine in this work, and the slope of this linear regression provided an estimation of factor B, defined as

$$B = \frac{16\pi\nu^2\gamma^3}{3k^3T^3} \tag{10}$$

https://doi.org/10.1021/acs.cgd.2c01229
Cryst. Growth Des. 2023, 23, 1668−1675

where ν is the volume of one molecule, γ represents the interfacial energy, k is the Boltzmann constant, and T is the absolute temperature in Kelvin.

Interfacial energy is the work required to generate a new interface between the supersaturated solution and the solid phase contacting it.[23] Critical radius r_C is the critical radius that corresponds to the minimum size at which a particle can survive in a solution without being redissolved.[24] Number of molecules in critical nucleus n_C is the number of molecules that must be included in the initial nucleus. Activation Gibbs energy ΔG_C is the energy barrier that the cluster needs to conquer to form a nucleus during the homogeneous nucleation process.[1] From the thermodynamic factor B, the interfacial energy γ and the following nucleation parameters can be calculated.[22]

Interfacial energy

$$\gamma = \left(\frac{3k^3T^3B}{16\pi\nu^2}\right)^{1/3} \tag{11}$$

Critical radius:.

$$r_C = \frac{2\nu\gamma}{RT\ \ln S} \tag{12}$$

Number of molecules in the critical nucleus

$$n_C = \frac{4\pi r_C^3}{3\nu} \tag{13}$$

Activation Gibbs energy

$$\Delta G_C = \frac{16\pi\gamma^3\nu^2}{3k^2T^2(\ln S)^2} \tag{14}$$

where ν is the volume of one molecule, S is the supersaturation, γ represents the interfacial energy, k is the Boltzmann constant, and T is the absolute temperature in Kelvin.

EXPERIMENTAL SECTION

The Solid-State Characterization of Glycine Homopeptides. PXRD patterns were collected by a PANalytical X'Pert PRO X-ray diffractometer. Samples were filtrated and pressed into the sample holder. At 40 kV and 40 mA, Cu Kα radiation (1.5405 Å) was used to accomplish the X-ray diffraction experiment. All samples were scanned at a rate of 1 step/s throughout a diffraction angle range of 2 to 50°.

Induction Time Measurement. The induction times of glycine homopeptides crystallization were determined in water at two different temperatures, 278.15 K and 283.15 K. Solutions with different supersaturation levels (listed in Table S2) were prepared for each glycine homopeptide in test tubes. For glycine and diglycine, 2 mL solutions were made with 2 g of deionized water, whereas a volume of 1.5 mL was preferred for triglycine due to the increased feasibility of nucleation. The tubes were equipped with a small magnetic stir bar and meticulously sealed with rubber lids wrapped with parafilm both inside and outside the cap. The samples were placed into the hot thermostat bath maintained at 333.15 K, well above the supersaturation temperature of glycine homopeptides. The solutions were stirred at 500 rpm in the water bath until all the glycine homopeptides had fully dissolved (Figure S1). The clear tubes were then immersed in a cold thermostat bath held at a low constant nucleation temperature (278.15 K and 283.15 K). During the experiment, the solutions of different supersaturations for each peptide were tested in parallel and continuously magnetically stirred at 250 rpm. The induction time was recorded as the time of the first observation of the solution becoming cloudy. Once the solutions had nucleated, the tubes were transferred back to the water bath held at a temperature above the supersaturation temperature, to dissolve before repeating the nucleation experiment cycle. Induction time data were obtained for 100 times for each glycine homopeptide and each supersaturation level to capture the stochastic nature of nucleation. After all the induction time measurements were performed, the solutions were filtered, and the powders were tested using PXRD to determine the morphology of the crystallized glycine homopeptides to make sure there was no polymorphism transformation during the nucleation process.

RESULTS AND DISCUSSION

The Solid-State Characterization of Glycine Homopeptides. Glycine homopeptides (glycine (α form), diglycine (α form), triglycine (β form), tetraglycine, pentaglycine, and hexaglycine) were supplied by Sigma-Aldrich Company Ltd. (Figure 1, Table S1) and were used as received. Deionized water was produced in the laboratory.

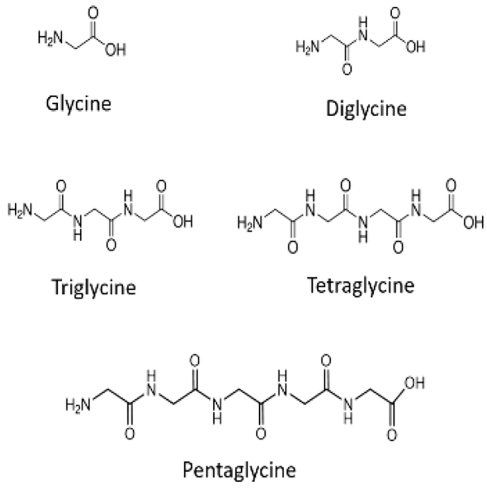

Figure 1. Chemical structures of glycine homopeptides.

The PXRD patterns of glycine homopeptides used in this work have been tested before and after the induction time measurement to make sure that there was no phase transition. As the examples show in Figure S2, all the samples kept the same XRD pattern, except triglycine. The new XRD patterns of triglycine are a result of the dihydrate morphology as reported previously.[16] The dihydrate form of triglycine can be obtained when the temperature is lower than 303.15 K.

The Nucleation Parameters of Glycine Homopeptides. The induction times of glycine, diglycine, triglycine, tetraglycine, pentaglycine, and hexaglycine were measured under 278.15 K at different supersaturation levels (1.5, 2, 3) in 2 mL of water. The images and SEM micrographs of the produced crystals are presented in Figure 2. The crystals of glycine homopeptides are all regularly shaped—rodlike for glycine, needle for triglycine dihydrate, plate for di, tetra-, penta-, and hexaglycine. The solution of pentaglycine and hexaglycine became cloudy after several days first until small crystals came out, and the induction time was longer than 1 week.

The experimental results present that the induction time increased with the increasing number of amino acid residues (Figure 3). Glycine has the shortest induction time, whereas pentaglycine has the longest induction time. Moreover, when

https://doi.org/10.1021/acs.cgd.2c01229
Cryst. Growth Des. 2023, 23, 1668−1675

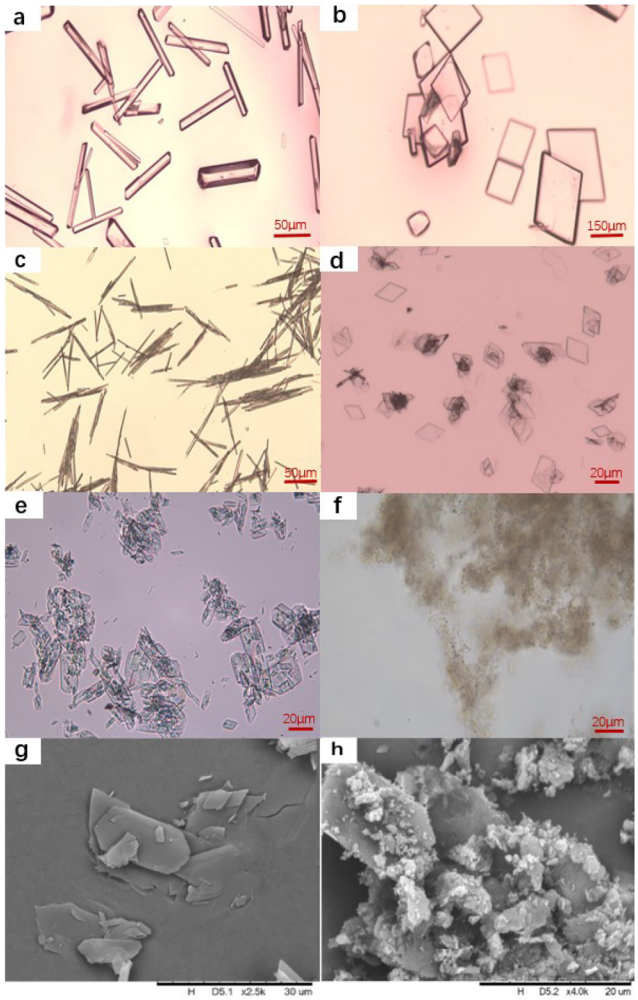

Figure 2. Microscope images of glycine homopeptides (a) glycine, (b) diglycine, (c) triglycine dihydrate, (d) tetraglycine, (e) pentaglycine, (f) hexaglycine, and SEM images of pentaglycine (g) and hexaglycine (h).

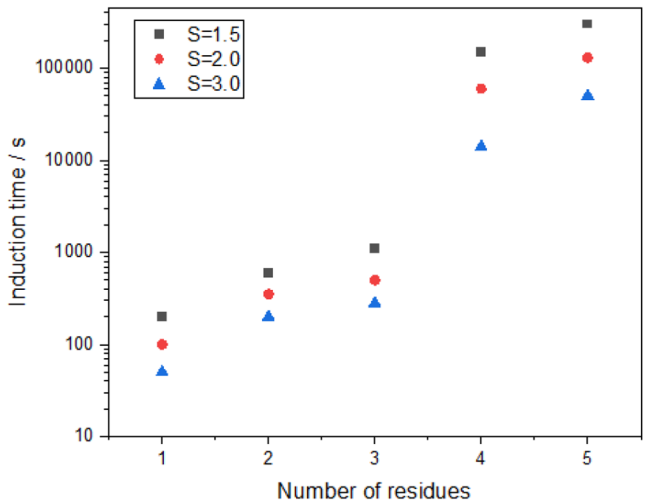

Figure 3. Induction time of glycine homopeptides under different supersaturation levels at 278.15 K.

the number of amino acids in glycine homopeptides exceeds three, the induction time increases by an order of magnitude, which also indicates that when the chain length is long enough, there is no linear relationship between the number of peptide bonds and the nucleation rate. Furthermore, the induction time decreased with the increase of the supersaturation level S.

In order to explore the effect of chain length and conformation on the nucleation process, the nucleation parameters of glycine, diglycine and triglycine dihydrate were calculated based on the stochastic nature of nucleation and were compared with each other. Figure 4 and Figure S4 present the probability distribution of the induction times for glycine, diglycine, and triglycine at 278.15 K and 283.15 K. The exponential based Poisson function (eq 3) was utilized to correlate the experimental data, of which the outcome is provided in Table S3. For various rate-limiting steps in the nucleation process, eqs 6−9 can be used to characterize the relationship between the nucleation rate and the supersaturation. The goodness of fit of these four functions was evaluated in order to identify which one best matched the experimental data, as shown in Figure S3. The best fitting findings (the lowest R^2 value) are provided by eq 9, indicating that the nucleation rate for glycine homopeptides in water is regulated by the interface transfer condition, and nucleus growth occurs via a surface nucleation process.

The relationship between $1/(\ln S)^2$ and $\ln J + 3\ln(\ln S)$ of glycine homopeptides in eq 9 are shown in Figure 5. From the intercept $\ln A$ and the slope B of each linear line, the pre-exponential factor A and the interfacial energy γ can be determined, respectively. Under same temperature, the steeper the slope, the larger the B, and the higher value of $\upsilon^2\gamma^3$. The activation Gibbs energy ΔG_C calculated using eq 14 became higher at the same supersaturation level, making the induction time longer. From the interfacial energy, the size of the critical nucleus r_C, the number of molecules n_C in the critical nucleus, and the free-energy barrier to nucleationΔG_C can be calculated by eqs 11−14. The values are listed in Table S4 and Table S5.

According to the results obtained in Tables S4 and S5, as the supersaturation level increases, the Gibbs free energy, critical radius, and number of molecules in one nucleus decrease. This relationship was seen across the different results of the same peptide in both temperatures of different chain lengths. This is potentially because the amount of energy required to form the earliest nucleus of critical size is lower at higher supersaturation levels, and hence, the induction time would be shorter.

The comparison of nucleation parameters between different peptides is shown in Figure 6. Crystals nucleate more rapidly with a shorter chain length; thus, glycine, which contains only one amino acid, nucleates the quickest and has the highest nucleation rate J, while triglycine dihydrate, which has three amino acid residues, nucleates the slowest and has the lowest nucleation rate J. The nucleation rate at 283.15 K is greater than that at 278.15 K, which could be because the molecules are more active at a higher temperature, resulting in a faster rate of surface integration and hence a faster nucleation rate.

The kinetics of the new phase transformation (from liquid to solid) process is determined by the surface free energy of the emerging phase boundary, and a greater difficulty in nucleation equals a higher solid−liquid interfacial energy.[13,23] The order of the interfacial energy of glycine homopeptides in water under the same temperature is as follows: glycine > diglycine > triglycine dihydrate. Triglycine dihydrate is supposed to have the highest γ as an increase in the number of amino acid residues, resulting in an increase in the difficulty of nucleation, but results do not align. From the definition of interfacial

https://doi.org/10.1021/acs.cgd.2c01229
Cryst. Growth Des. 2023, 23, 1668−1675

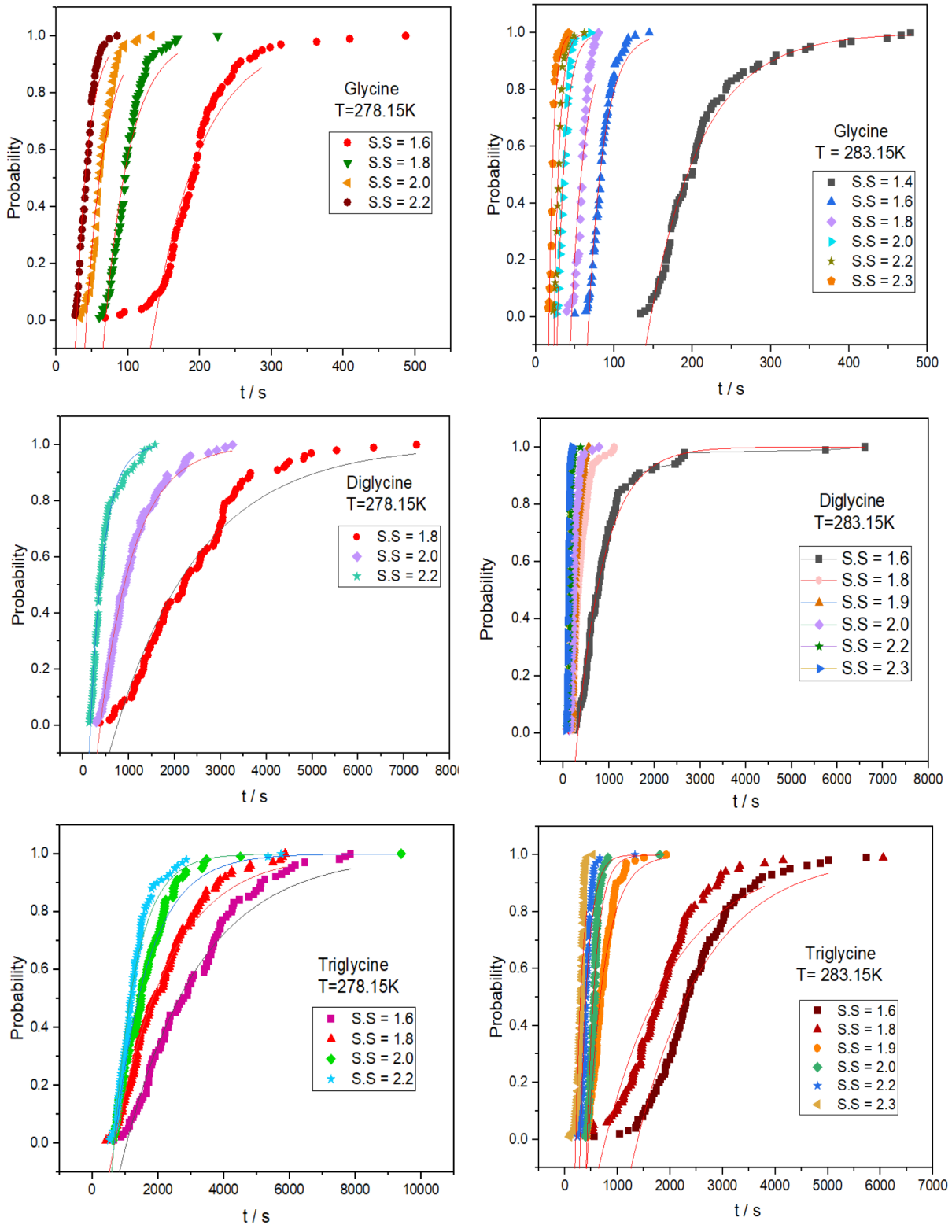

Figure 4. Induction time of glycine homopeptides under different supersaturation levels at 278.15 K and 283.15 K (the Poisson distribution is represented by solid lines with a good fit).

energy, it is proportional to thermodynamic factor B and inversely proportional to the volume of one peptide molecule. The interfacial energy of various peptides at the same temperature is incomparable because of the different molecular volumes. Since the order of molecular volume is triglycine dihydrate > diglycine > glycine, the order of B is diglycine > glycine > triglycine dihydrate at 278.15 K, and triglycine dihydrate > diglycine > glycine at 283.15 K, so triglycine dihydrate can adopt the lowest interfacial energy compared with glycine and diglycine. The influence of temperature on

https://doi.org/10.1021/acs.cgd.2c01229
Cryst. Growth Des. 2023, 23, 1668−1675

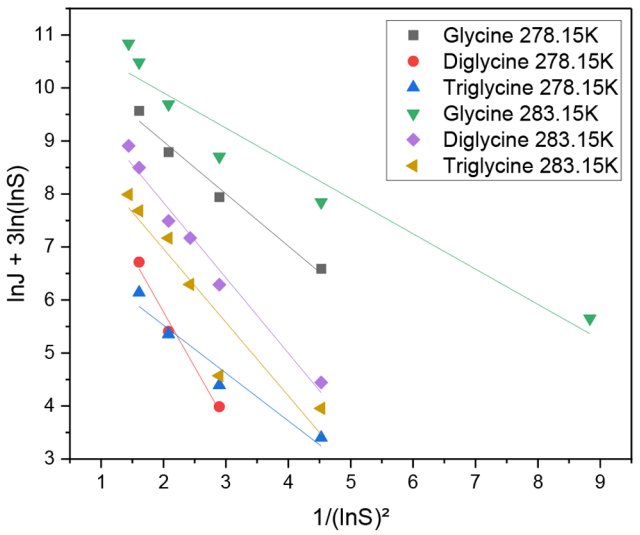

Figure 5. Comparison of the relationships between the nucleation rate and supersaturation level of glycine homopeptides under different temperatures.

the interfacial energy, on the other hand, can be investigated. When the temperature is increased, all the interfacial energies become lower, except for triglycine dihydrate. However, the induction time of triglycine dihydrate is shorter than that at a lower temperature, which means the interfacial energy of triglycine dihydrate cannot be used as the only evidence of whether the nucleation rate is high or not.

From Figure 6, for all peptides and temperatures, as supersaturation increases, ΔG_C decreases, indicating that higher driving force accelerates nucleation. When investigating the effect of chain length on activation energy, the energy at the same supersaturation level and temperature was compared. When the temperature is 283.15 K, triglycine dihydrate has the largest ΔG_C and longest induction time, which aligns with the trend of activation energy. When the temperature is lower as 278.15 K, triglycine has the lowest activation energy compared with mono- and diglycine, which is contradictory with its longest induction time. For mono- and diglycine, ΔG_C decreases when the temperature is higher, while for triglycine dihydrate, the ΔG_C increases when the temperature is higher. However, the induction time of triglycine dihydrate is shorter at the higher temperature. Based on our previous research, triglycine will form dihydrate at temperatures below 303 K with the unfolded pPII conformation, while it will convert to anhydrate at higher temperatures with the almost fully extended conformation.[16] The Ramachandra plot reveals that both the pPII and β-sheet conformations have a strong preference over other alternative conformations in solution at 278 K. The predominance of pPII conformation diminishes as the temperature increases until the conformation is converted to a β-sheet in anhydrate form. For triglycine dihydrate, the unfolded conformation with extra hydrogen bonds formed at a lower temperature, which is not stable with the temperature increasing, causing a higher calculated ΔG_C. In summary, the flexible conformation at varying temperatures rendered the traditional nucleation theory inapplicable to triglycine dihydrate.

Apart from the classical nucleation theory, other nonclassical nucleation models have been developed over the last two decades.[11,25−29] For the glycine homopeptides, the liquid−liquid phase separation was also observed for hexaglycine before the nucleation, which can be seen in Figure 7d,e. The

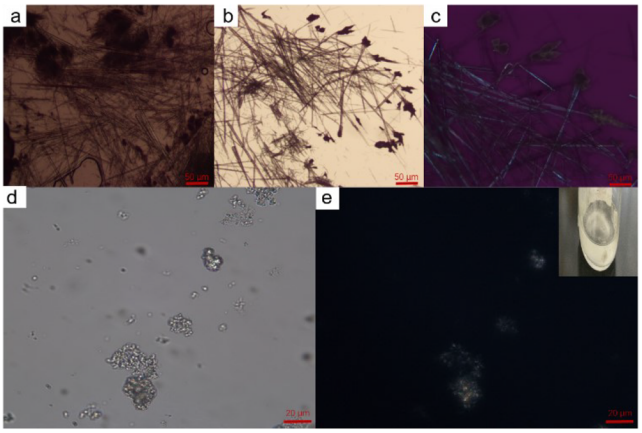

Figure 7. Gelation phenomenon of triglycine dihydrate nucleation captured by an optical microscope (a, b) and polarizing microscope (c) and liquid−liquid phase separation of hexaglycine nucleation captured by an optical microscope (d) and polarizing microscope (e).

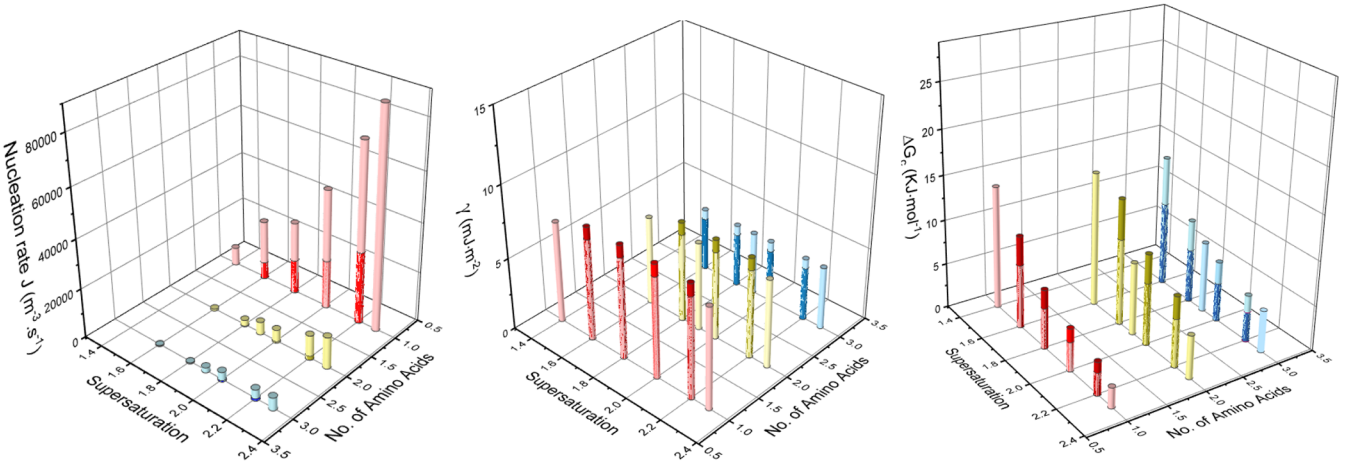

Figure 6. Relationship between nucleation rate J, interfacial energy γ, activation energy ΔG_C supersaturation levels, and the number of glycine residues. The darker color represents the results at 278.15 K, whereas the lighter color means the results at 283.15 K.

https://doi.org/10.1021/acs.cgd.2c01229
Cryst. Growth Des. 2023, 23, 1668−1675

solution became blurry first, and there were some gel-like particles that will not settle for a long time, similar to the liquid–liquid separation process observed in the literatures.[30,31]

For triglycine, gelation appeared during the crystallization of triglycine dihydrate (Figure 7a–c). This discovery raises a question whether there is any relationship between gelation and liquid–liquid separation during the peptide crystallization. However, because the solubility of hexaglycine is very low, the gelation is difficult to observe. This observation can be further explored to study the nucleation mechanism for longer chain peptides.

CONCLUSION

In summary, the nucleation of glycine homopeptides was investigated in this work to explore the effect of chain length and conformation on the nucleation mechanism of short chain homopeptides. The induction time increases with the peptide chain length, which even exhibits an exponential increase when the number of glycine residues exceeds three. For the glycine, diglycine and triglycine, the nucleation parameters (nucleation rate J, growth time t_g, interfacial energy γ, critical radius r_C, number of molecules in critical nucleus n_C and activation Gibbs energy ΔG_C) were calculated. With increasing supersaturation, activation energy, critical radius, number of molecules and growth time decrease, while the nucleation rate increases for all homopeptides. Lower temperature makes the nucleation more difficult and the induction time longer. When the temperature is lower, the interfacial energy γ and Gibbs energy ΔG_C are higher for glycine and diglycine. However, for triglycine, the dihydrate with unfolded conformation was formed during the nucleation process, and the values of interfacial energy and Gibbs energy at low temperature are both lower than those at high temperature, which means the classical nucleation theory is not suitable to explain the nucleation phenomenon of triglycine dihydrate. Moreover, the gelation phenomenon of triglycine dihydrate was found during the nucleation process, as well as the liquid–liquid separation of hexaglycine. For glycine homopeptides, nonclassical nucleation theory provides a better explanation when the chain length is longer than three with more flexible conformation in solution. This work gives a better understanding of the nucleation mechanism for different chain length peptides.

ASSOCIATED CONTENT

Supporting Information

The Supporting Information is available free of charge at https://pubs.acs.org/doi/10.1021/acs.cgd.2c01229.

Details of the experimental setup, XRD patterns, induction time, the calculated nucleation kinetics parameters, Tables S1–S4, and Figures S1–S4 (PDF)

AUTHOR INFORMATION

Corresponding Author

Jerry Y. Y. Heng – *Department of Chemical Engineering and Institute for Molecular Science and Engineering, Imperial College London, London SW7 2AZ, U.K.;* orcid.org/0000-0003-2659-5500; Email: jerry.heng@imperial.ac.uk

Authors

Mingxia Guo – *Department of Chemical Engineering, Imperial College London, London SW7 2AZ, U.K.;* orcid.org/0000-0001-5957-5915

Marie J. Jones – *Department of Chemical Engineering, Imperial College London, London SW7 2AZ, U.K.;* orcid.org/0000-0002-6018-9656

Racheal Goh – *Department of Chemical Engineering, Imperial College London, London SW7 2AZ, U.K.*

Vivek Verma – *Department of Chemical Engineering, Imperial College London, London SW7 2AZ, U.K.;* orcid.org/0000-0001-9635-8346

Emily Guinn – *Synthetic Molecule Design and Development, Lilly Research Laboratories, Eli Lilly and Company, Indianapolis, Indiana 46221, United States*

Complete contact information is available at: https://pubs.acs.org/10.1021/acs.cgd.2c01229

Author Contributions

Mingxia Guo: Conceptualization, Methodology, Investigation, Formal analysis, Writing–review and editing. Marie J. F. Jonesa: Investigation, Racheal Goh: Investigation, Vivek Verma: Writing–review and editing, Emily Guinn: Writing–review and editing, Jerry Y. Y. Heng: Supervision, Funding acquisition, Project administration, Conceptualization.

Notes

The authors declare no competing financial interest.

ACKNOWLEDGMENTS

We are grateful for the financial support from the Engineering and Physical Science Research Council of the UK via Prosperity Partnership (EP/N015916/1, EP/T005556/1, and EP/T518207/1) and the Eli Lilly and Company. M.G. acknowledges the China Scholarship Council (CSC) for funding her Ph.D.

REFERENCES

(1) Karthika, S.; Radhakrishnan, T. K.; Kalaichelvi, P. A Review of Classical and Nonclassical Nucleation Theories. *Cryst. Growth Des.* **2016**, *16* (11), 6663–6681.

(2) Ostergaard, I.; Szilagyi, B.; de Diego, H. L.; Qu, H.; Nagy, Z. K. Polymorphic Control and Scale-Up Strategy for Antisolvent Crystallization Using Direct Nucleation Control. *Cryst. Growth Des.* **2020**, *20* (4), 2683–2697.

(3) Hwang, H.; Cho, Y. C.; Lee, S.; Lee, Y. H.; Kim, S.; Kim, Y.; Jo, W.; Duchstein, P.; Zahn, D.; Lee, G. W. Hydration Breaking and Chemical Ordering in A levitated NaCl Solution Droplet Beyond the Metastable Zone Width Limit: Evidence for the Early Stage of Two-Step Nucleation. *Chem. Sci.* **2021**, *12* (1), 179–187.

(4) Tsarfati, Y.; Rosenne, S.; Weissman, H.; Shimon, L. J. W.; Gur, D.; Palmer, B. A.; Rybtchinski, B. Crystallization of Organic Molecules: Nonclassical Mechanism Revealed by Direct Imaging. *ACS Cent. Sci.* **2018**, *4* (8), 1031–1036.

(5) Kulkarni, S. A.; Kadam, S. S.; Meekes, H.; Stankiewicz, A. I.; ter Horst, J. H. Crystal Nucleation Kinetics from Induction Times and Metastable Zone Widths. *Cryst. Growth Des.* **2013**, *13* (6), 2435–2440.

(6) Kaissaratos, M.; Filobelo, L.; Vekilov, P. G. Two-Step Crystal Nucleation Is Selected Because of a Lower Surface Free Energy Barrier. *Cryst. Growth Des.* **2021**, *21* (9), 5394–5402.

(7) Gebauer, D.; Kellermeier, M.; Gale, J. D.; Bergstrom, L.; Colfen, H. Pre-nucleation clusters as solute precursors in crystallisation. *Chem. Soc. Rev.* **2014**, *43*, 2348.

(8) Weissbuch, I.; Lahav, M.; Leiserowitz, L. Toward Stereochemical Control, Monitoring, and Understanding of Crystal Nucleation. *Cryst. Growth Des.* **2003**, *3* (2), 125−150.
(9) Vekilov, P. G.; Vorontsova, M. A. Nucleation Precursors in Protein Crystallization. *Acta Crystallogr. F:Struct. Biol. Commun.* **2014**, *70*, 271−282.
(10) Galkin, O.; Vekilov, P. G. Control of Protein Crystal Nucleation Around the Metastable Liquid−Liquid Phase Boundary. *Proc. Natl. Acad. Sci. U.S.A.* **2000**, *97* (12), 6277−6281.
(11) Li, X.; Wang, J.; Wang, T.; Wang, N.; Zong, S.; Huang, X.; Hao, H. Molecular Mechanism of Crystal Nucleation from Solution. *Sci. China Chem.* **2021**, *64*, 1460−1481.
(12) Vekilov, P. G. Dense Liquid Precursor for the Nucleation of Ordered Solid Phases from Solution. *Cryst. Growth Des.* **2004**, *4*, 671−685.
(13) Vekilov, P. G. Nucleation. *Cryst. Growth Des.* **2010**, *10* (12), 5007−5019.
(14) Gebauer, D.; Kellermeier, M.; Gale, J. D.; Bergstrom, L.; Colfen, H. Pre-nucleation Clusters as Solute Precursors in Crystallisation. *Chem. Soc. Rev.* **2014**, *43* (7), 2348−71.
(15) Guo, M.; Chang, Z. H.; Liang, E.; Mitchell, H.; Zhou, L.; Yin, Q.; Guinn, E. J.; Heng, J. Y. Y. The Effect of Chain Length and Side Chains on the Solubility of Peptides in Water from 278.15 to 313.15 K: A Case Study in Glycine Homopeptides and Dipeptides. *J. Mol. Liq.* **2022**, *352*, 118681.
(16) Guo, M.; Rosbottom, I.; Zhou, L.; Yong, C. W.; Zhou, L.; Yin, Q.; Todorov, I. T.; Errington, E.; Heng, J. Y. Y. Triglycine (GGG) Adopts a Polyproline II (pPII) Conformation in Its Hydrated Crystal Form: Revealing the Role of Water in Peptide Crystallization. *J. Phys. Chem. Lett.* **2021**, *12*, 8416−8422.
(17) Bernardo, A.; Calmanovici, C. E.; Miranda, E. A. Induction Time as an Instrument to Enhance Comprehension of Protein Crystallization. *Cryst. Growth Des.* **2004**, *4* (4), 799−805.
(18) Jiang, S.; ter Horst, J. H. Crystal Nucleation Rates from Probability Distributions of Induction Times. *Cryst. Growth Des.* **2011**, *11* (1), 256−261.
(19) Sohnel, O.; Mullin, J. W. Interpretation of Crystallization Induction Periods. *J. Colloid Interface Sci.* **1988**, *123* (1), 43−50.
(20) Davey, R. J.; Schroeder, S. L.; ter Horst, J. H. Nucleation of organic crystals–a molecular perspective. *Angew. Chem., Int. Ed. Engl.* **2013**, *52* (8), 2166−2179.
(21) Dunning, W. J.; Notley, N. T. Kinetics of Crystallization. III. *Zeitschrift für Elektrochemie, Berichte der Bunsengesellschaft für physikalische Chemie* **1957**, *61*, 55−59.
(22) Yang, Y.; Zhou, L.; Zhang, X.; Yang, W.; Zhang, S.; Xiong, L.; Wei, Y.; Zhang, M.; Hou, B.; Yin, Q. Influence of solvent properties and intermolecular interaction between solute and solvent on nucleation kinetics of HMBTAD. *J. Cryst. Growth* **2018**, *498*, 77−84.
(23) Omar, W.; Mohnicke, M.; Ulrich, J. Determination of the solid liquid interfacial energy and thereby the critical nucleus size of paracetamol in different solvents. *Cryst. Res. Technol.* **2006**, *41* (4), 337−343.
(24) Thanh, N. T. K.; Maclean, N.; Mahiddine, S. Mechanisms of Nucleation and Growth of Nanoparticles in Solution. *Chem. Rev.* **2014**, *114* (15), 7610−7630.
(25) Dighe, A. V.; Podupu, P. K. R.; Coliaie, P.; Singh, M. R. Three-Step Mechanism of Antisolvent Crystallization. *Cryst. Growth Des.* **2022**, *22*, 3119−3127.
(26) Chen, H. L.; Li, M. L.; Lu, Z. Y.; Wang, X. G.; Yang, J. S.; Wang, Z.; Zhang, F.; Gu, C. H.; Zhang, W. N.; Sun, Y. J.; Sun, J. L.; Zhu, W. G.; Guo, X. F. Multistep nucleation and growth mechanisms of organic crystals from amorphous solid states. *Nat. Commun.* **2019**, *10*, 3872.
(27) Karthika, S.; Radhakrishnan, T. K.; Kalaichelvi, P. A Review of Classical and Nonclassical Nucleation Theories. *Cryst. Growth Des.* **2016**, *16*, 6663−6681.
(28) Mirabello, G.; Ianiro, A.; Bomans, P. H. H.; Yoda, T.; Arakaki, A.; Friedrich, H.; de With, G.; Sommerdijk, N. J. M. Crystallization by particle attachment is a colloidal assembly process. *Nat. Mater.* **2020**, *19* (4), 391−396.
(29) Loh, N. D.; Sen, S.; Bosman, M.; Tan, S. F.; Zhong, J.; Nijhuis, C. A.; Kral, P.; Matsudaira, P.; Mirsaidov, U. Multistep nucleation of nanocrystals in aqueous solution. *Nat. Chem.* **2017**, *9* (1), 77−82.
(30) Wang, Y.; Lomakin, A.; Kanai, S.; Alex, R.; Benedek, G. B. Liquid-Liquid Phase Separation in Oligomeric Peptide Solutions. *Langmuir* **2017**, *33* (31), 7715−7721.
(31) Yuan, C.; Levin, A.; Chen, W.; Xing, R.; Zou, Q.; Herling, T. W.; Challa, P. K.; Knowles, T. P. J.; Yan, X. Nucleation and Growth of Amino Acid and Peptide Supramolecular Polymers through Liquid-Liquid Phase Separation. *Angew. Chem., Int. Ed. Engl.* **2019**, *58* (50), 18116−18123.

https://doi.org/10.1021/acs.cgd.2c01229
Cryst. Growth Des. 2023, 23, 1668−1675